

Effectiveness of rf phase modulation for increasing bunch length in electron storage rings

F. Orsini and A. Mosnier

CEA Saclay, Bâtiment 701, 91191 Gif-sur-Yvette, France

(Received 25 March 1999)

Aiming at increasing the apparent bunch length and hence the beam lifetime in electron storage rings, rf phase modulation near one parametric resonance has been experimentally investigated. Since the possible benefit of this technique depends greatly on the ring parameters, we studied the effect of such a modulation for different rf parameters on the longitudinal emittance. Theoretical predictions and results of simulations are compared and discussed. It is shown that synchrotron radiation tends to spoil the parametric resonance. In particular, a criterion for island survival has been found.

PACS number(s): 29.20.-c, 29.27.-a, 41.60.-m

I. INTRODUCTION

In order to reach very high brilliance, synchrotron radiation light sources demand intense bunches with very small transverse and longitudinal emittances. However, the high density of electrons increases the Touschek effect (e^-e^- collisions at large angle) and thus reduces the beam lifetime. In order to reduce the electron density, different approaches have been considered: a higher harmonic cavity operating in the bunch lengthening mode or a rf phase modulation [1], which increases the apparent bunch length but also the energy spread of the beam. This paper focuses on the second method, especially near the third-integer resonance, more appropriate than the integer resonance. The latter, widely explained in previous papers [2], is too strong to be useful in storage rings—distinct bunchlets with large spacing are formed—and is briefly discussed in Sec. II. The third-integer resonance, more promising, can be controlled through the two modulation parameters frequency ω_m and amplitude A_m , which must first be properly chosen. Analytical expressions for fixed points and island widths are given in Sec. III and help for the optimization of the modulation. For illustration, three synchrotron light sources are compared: BESSY I, SOLEIL, and SuperACO. Lastly, the combined effect of both synchrotron radiation and parametric resonance is studied in Sec. IV. Islands created by rf modulation tend to vanish as soon as radiation damping is introduced. A criterion that guarantees island formation is then inferred from the Fokker-Planck equation. The validity of the criterion is finally tested with different parameters of the three machines.

II. INTEGER RESONANCE

The integer resonance has been thoroughly analyzed in [2]. The particle motion can be characterized by three regimes according to the value of the modulation tune, with respect to a bifurcation frequency, given by

$$\omega_c = \omega_s \left[1 - \frac{3}{16} (4A_m)^{2/3} \right],$$

with ω_s the synchrotron frequency and A_m the amplitude of the perturbation of the first harmonic.

Well below the bifurcation frequency ω_c , two stable fixed points (SFP's) define two well separated domains, which particles fill in about the same proportions. Above ω_c , only the farthest stable fixed point is left and the particles diffuse toward this off-centered island.

The three regimes of the integer resonance have been simulated with the parameters of the SOLEIL storage ring. Figure 1 shows, for example, the gathering of particles, initially uniformly distributed in phase space, into the islands after a few damping times for different modulation tunes. As soon as the modulation amplitude is large enough so that the integer resonance takes place, dipole oscillations of large magnitude are created, whatever the regime. The integer parametric resonance is definitely not an appropriate method for decreasing the electron density of the bunch.

III. THIRD-INTEGERS RESONANCE

A. Hamiltonian of the third-integer resonance: $\omega_m \approx 3\omega_s$

Only the main results are recalled hereafter and detailed derivations can be found in the Appendix. We consider a phase modulation with frequency close to three times the synchrotron frequency. The complete perturbed Hamiltonian, as a function of the phase ϕ and the energy deviation δ of one particle, can be written as

$$\begin{aligned} H(\phi, \delta) = & \frac{\omega_s}{2} \delta^2 + \omega_s \tan \overline{\phi_s} [\sin \phi \cos(A_m \sin \omega_m t) \\ & + \cos \phi \sin(A_m \sin \omega_m t)] \\ & - \omega_s \cos \phi \cos(A_m \sin \omega_m t) \\ & + \omega_s \sin \phi \sin(A_m \sin \omega_m t) - \omega_s \phi \tan \overline{\phi_s}, \quad (1) \end{aligned}$$

where ω_s is the synchrotron frequency and we define $\overline{\phi_s} = \pi - \phi_s$ with ϕ_s the synchronous angle.

We examine the Hamiltonian in the coordinate frame, rotating at the modulation frequency, by using the action-angle variables $(\tilde{J}, \tilde{\psi})$ defined as

$$\delta = -\sqrt{2\tilde{J}} \cos(\tilde{\psi} + \omega_m t/3), \quad \phi = -\sqrt{2\tilde{J}} \sin(\tilde{\psi} + \omega_m t/3).$$

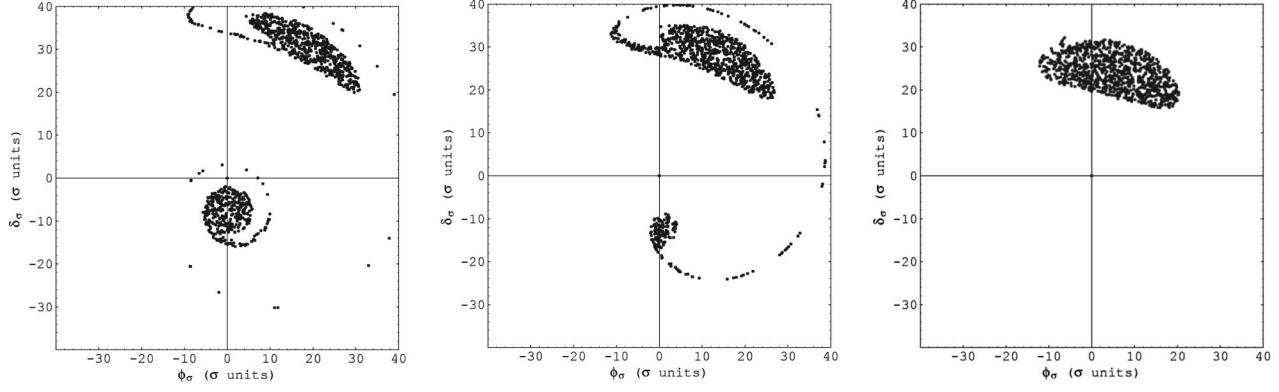


FIG. 1. Particles in normalized phase space (ϕ, δ) with rf phase modulation at the integer resonance. (a) Well below the bifurcation frequency; (b) just below the bifurcation frequency; (c) above the bifurcation frequency.

Expanding into Bessel functions and assuming that we are close to the third-integer parametric resonance, the time-averaged Hamiltonian, representing the motion invariant, takes the simple form

$$\langle K \rangle_t = \left(\omega_s - \frac{\omega_m}{3} \right) \tilde{J} - \frac{\omega_s \tilde{J}^2}{16} - \frac{\omega_s A_m (2\tilde{J})^{3/2}}{48} \cos 3\tilde{\psi} - \omega_s. \quad (2)$$

In addition to the first linear term of the third-integer resonance, the Hamiltonian includes higher order functions of \tilde{J} . The cosine term provides the $\tilde{\psi}$ periodicity of $2\pi/3$. The terms like ω_s that do not depend on \tilde{J} and $\tilde{\psi}$ do not affect the differential equations and hence can be ignored. In the new phase space variables $(\tilde{J}, \tilde{\psi})$, the stationary trajectories are given by the K -constant contours.

The position and width of the three islands, which determine the phase space occupied by the beam, are controlled by the modulation parameters and must be properly adjusted.

B. Fixed points

The coordinates $(\phi_\sigma, \delta_\sigma)$ of the three stable fixed points are (for $\tilde{\psi} = 0, 2\pi/3, 4\pi/3$)

$$\delta_\sigma = \frac{a_m}{2}(1 + R_{FP}), \quad -\frac{a_m}{4}(1 + R_{FP}), \quad -\frac{a_m}{4}(1 + R_{FP}),$$

$$\phi_\sigma = 0, \quad \sqrt{3} \frac{a_m}{4}(1 + R_{FP}), \quad -\sqrt{3} \frac{a_m}{4}(1 + R_{FP}), \quad (3)$$

with the factor $R_{FP} = \frac{1}{\sqrt{1 + (64Q_s^2/a_m^2)(\sigma_\epsilon h \alpha)^2(1 - \omega_m/3\omega_s)}}$, where a_m is the normalized modulation amplitude (A_m is in units of rms bunch length), Q_s is the synchrotron tune, σ_ϵ is the natural energy spread, α is the momentum compaction, and h is the harmonic number.

The fixed point position depends on ring and rf modulation parameters. In order to depopulate the bunch center as much as possible, islands have to be large enough, on one hand, and be placed close to the bunch core, on the other hand. However, Eq. (3) shows that the stable fixed points can never reach the origin, even for a vanishing distance to the

resonance ($\omega_m - 3\omega_s$), and are bounded by the lower limit a_m . Figure 2 illustrates this limit.

C. Island width

The island width is given by the distance between the separatrices, the curves joining the unstable fixed points, and the stable fixed points, where the Hamiltonian is maximum [3]. The normalized width (in σ units) expressed in terms of storage ring parameters is given by

$$\Delta \delta_\sigma = \pm 16 \sqrt{\frac{2}{3}} \left(\frac{Q_s}{\alpha \sigma_\epsilon h} \right)^{3/2} (1 - \omega_m/3\omega_s)^{3/4} \frac{1}{\sqrt{a_m R_{FP}}}. \quad (4)$$

The K -constant contours, calculated for the SOLEIL ring, are shown in Fig. 3. At small amplitude, the motion is almost unaffected by the resonance. Moving away from the origin, the circles become more and more distorted, until reaching the islands. The expression (4) reveals that the more ω_m tends to $3\omega_s$, the more the island width is reduced. The width is drawn in Fig. 4 as a function of the distance to the resonance and scales as the power $\frac{1}{4}$. There is then a trade-

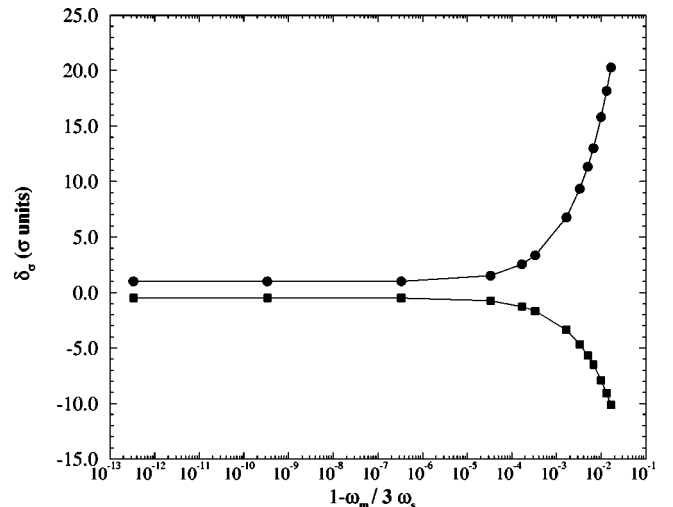


FIG. 2. SOLEIL: Evolution of the amplitude δ_σ of the stable fixed point versus the third-integer resonance coefficient $(1 - \omega_m/3\omega_s)$.

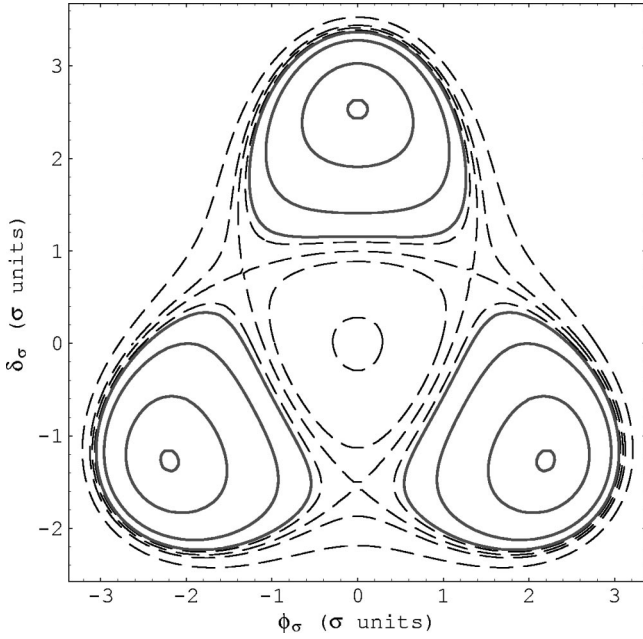


FIG. 3. K -constant contours plotted in normalized phase space (ϕ, δ) for SOLEIL ring parameters (curves surrounding the stable fixed points are in solid lines and curves surrounding the unstable fixed points are in dashed lines).

off between island position (ω_m very close to $3\omega_s$) and island width (ω_m not too close to $3\omega_s$).

D. Chirikov criterion

The Chirikov criterion [4] is used to estimate the onset of stochastic instability. In particular, chaotic behavior can occur when islands of two successive parametric resonances are too close and the overlap of resonances begins when their separatrices are in contact. As we will see later, this chaotic motion has been observed in some simulations with SOLEIL parameters.

The Chirikov criterion is given by [4]

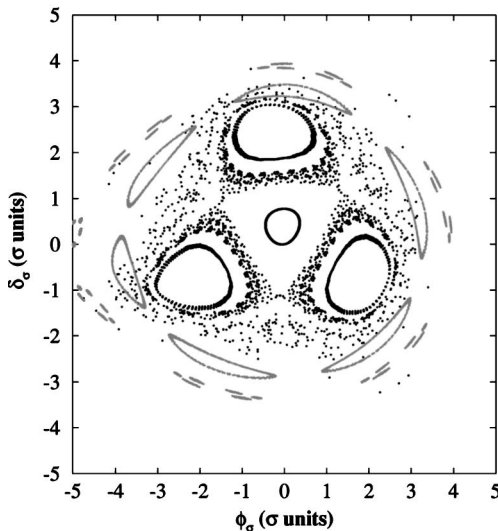


FIG. 5. Single bunch tracking in normalized phase space $(\phi_\sigma, \delta_\sigma)$. Dark points represent the third-integer resonance effect, gray points represent the fifth-integer resonance effect.

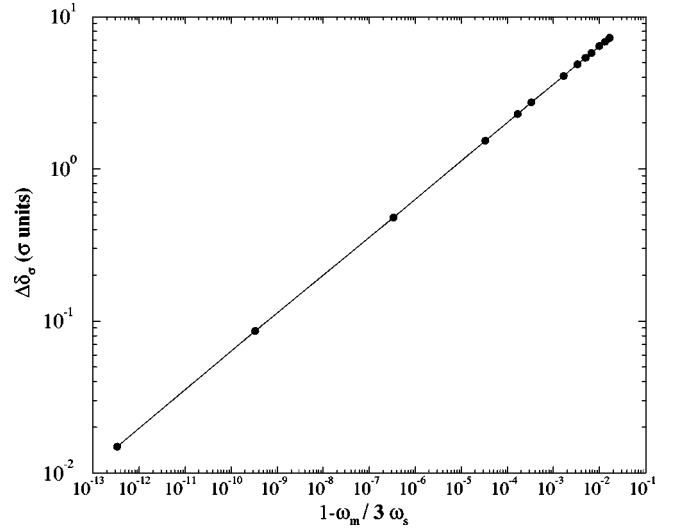


FIG. 4. $\Delta \delta_\sigma$ in σ units versus the modulation frequency coefficient $(1 - \omega_m/3\omega_s)$.

$$\Delta \tilde{J}_1 + \Delta \tilde{J}_2 \ll \delta \tilde{J}, \tag{5}$$

where $\Delta \tilde{J}_1$ and $\Delta \tilde{J}_2$ are the island widths of the third-integer and fifth-integer resonances, respectively, and $\delta \tilde{J}$ is the island spacing in amplitude.

In the case of rf phase modulation, and possible interaction between the third- and fifth- integer resonances, the criterion becomes

$$\left(\frac{A_m}{6}\right)^{1/2} \left(1 - \frac{\omega_m}{3\omega_s}\right)^{3/4} \ll \frac{\Delta \omega_s}{\omega_s},$$

with $\Delta \omega_s / \omega_s = 1/6m^2$ and $m=3$ for the third-integer resonance.

Expressed in terms of the normalized modulation amplitude, the condition on the modulation tune for nonchaotic behavior can be written as

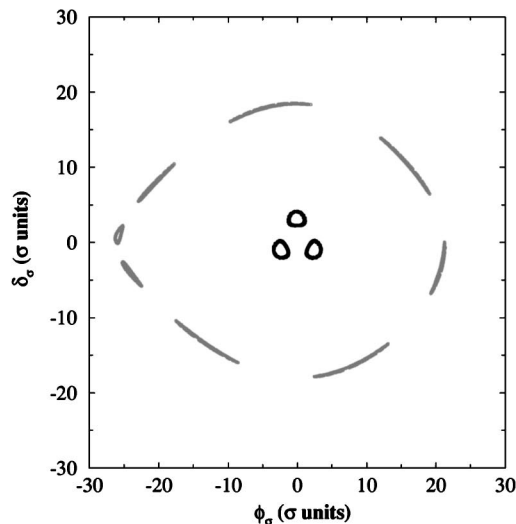


TABLE I. Synchrotron light sources' main parameters.

	SOLEIL	BESSY I	SuperACO
Frequency (MHz)	352.2	499.2	100.0
Harmonic number	396	104	24
Momentum compaction	4.77×10^{-4}	1.5×10^{-2}	1.48×10^{-2}
Nominal energy (MeV)	2500	800	800
Energy loss/turn (keV)	800	20	21.3
Total rf voltage (MV)	3.8	0.2	0.17
Longitudinal damping time (ms)	4.33	10.0	8.5
Natural energy spread	9.24×10^{-4}	5.0×10^{-4}	5.5×10^{-4}
Bunchlength/wavelength, σ_L/λ_{RF} (%)	2	7.9	4.5

$$\frac{\omega_m}{\omega_s} \gg 3 \left\{ 1 - \left[\frac{1}{54} \left(\frac{6\omega_s}{\omega_{RF}\alpha\sigma_\epsilon a_m} \right)^{1/2} \right]^{4/3} \right\}. \quad (6)$$

Figure 5 reproduces two numerical simulations for SOLEIL (chaotic behavior) and BESSY I (nonchaotic behavior). In nonchaotic behavior, the fifth-integer resonance has islands very far from the third-integer one, more than 15σ [Fig. 5(b)] with widths small in comparison to the island spacing. The particles are then independently governed by each resonance. Conversely, the fifth-integer islands hit the separatrices of the third-integer islands in the case of chaotic behavior [Fig. 5(a)]. The particles can then diffuse from one resonance to the next, leading to particle loss.

E. Optimization of the rf phase modulation parameters

The modulation parameters, frequency ω_m and amplitude A_m , have first been optimized with the help of the analytical expressions (3) and (4), together with different storage ring parameters [5]. Table I summarizes the relevant parameters used for three light sources: SOLEIL, BESSY I, and SuperACO.

Both the parameters, amplitude A_m and frequency ω_m of rf phase modulation, are given in Table II after optimization. The corresponding stationary trajectories are plotted in Fig. 6. It is worth noting that the a_m value is moderate for preventing any coherent motion of the whole bunch and that the fixed points are close enough to the bunch core, while keeping a sufficient island width.

When the bunch is short compared to the rf wavelength, especially for SOLEIL, the modulation frequency has to be moved very close to $3\omega_s$ in order to draw the fixed points to the origin. With these optimized parameters, we note that particles initially located at 1σ will be drawn out up to

nearly 3σ for the three machines. A significant bunch lengthening is therefore expected.

IV. SYNCHROTRON RADIATION EFFECT

In the previous analytical treatment, the synchrotron radiation effect, including radiation damping and quantum excitation, has not been taken into account. However, this effect cannot be neglected in storage rings, where these terms can be as large as the parametric resonance terms.

A. Fokker-Planck treatment

Due to the dissipative nature of the system, the previous Hamiltonian treatment cannot be directly applied in the presence of synchrotron radiation. The present analysis is based on the Vlasov equation with the Fokker-Planck collision term,

$$\frac{\partial F}{\partial t} + \{H, F\} = R, \quad (7)$$

where $F(\phi, \delta, t)$ is the distribution function of particles in the bunch, $R = (\partial/\partial\delta)(\gamma_d F \delta + \kappa \partial F/\partial\delta)$ is the collision term describing the synchrotron radiation effect, and $\{\dots\}$ denotes the Poisson bracket term. $\gamma_d = 1/T_{rad}$ is the radiation damping rate and κ is the quantum diffusion factor, related to γ_d by $\sigma_\epsilon = \sqrt{\kappa/\gamma_d}$.

With the help of the four partial derivatives

$$\frac{\partial \tilde{J}}{\partial \delta} = -\sqrt{2\tilde{J}} \cos \tilde{\psi}, \quad \frac{\partial \tilde{J}}{\partial \phi} = -\sqrt{2\tilde{J}} \sin \tilde{\psi},$$

TABLE II. Final optimization of the rf phase modulation parameters and island characteristics for each machine.

	SOLEIL	BESSY I	SuperACO
ω_m/ω_s	2.9995	2.9850	2.9950
A_m (deg)	1.48	5.68	3.24
SFP coordinates	(0, +2.54)	(0, +3.39)	(0, +3.43)
$(\phi_\sigma, \delta_\sigma)$	(+2.20, -1.27)	(+2.94, -1.69)	(+2.97, -1.71)
	(-2.20, -1.27)	(-2.94, -1.69)	(-2.97, -1.71)
Island width (σ units)	2.29	2.71	2.77

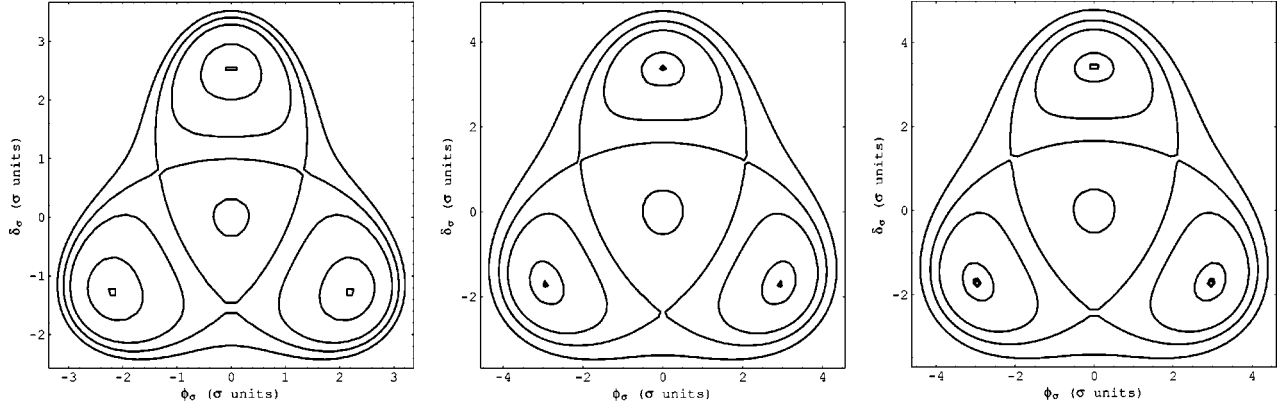


FIG. 6. Separatrices and K -constant contours in normalized phase space $(\phi_\sigma, \delta_\sigma)$ with rf phase modulation of the third integer. (a) SOLEIL; (b) BESSY I; (c) SuperACO.

$$\frac{\partial \tilde{\psi}}{\partial \delta} = -\frac{\sin \tilde{\psi}}{\sqrt{2\tilde{J}}}, \quad \frac{\partial \tilde{\psi}}{\partial \phi} = -\frac{\cos \tilde{\psi}}{\sqrt{2\tilde{J}}},$$

the new Fokker-Planck equation, in terms of $(\tilde{J}, \tilde{\psi})$ variables, is

$$\frac{\partial F}{\partial t} + \frac{\partial F}{\partial \tilde{\psi}} \frac{\partial K}{\partial \tilde{J}} - \frac{\partial F}{\partial \tilde{J}} \frac{\partial K}{\partial \tilde{\psi}} = 2 \frac{\partial}{\partial \tilde{J}} \left(\gamma_d \tilde{J} F + \kappa \tilde{J} \frac{\partial F}{\partial \tilde{J}} \right) \quad (8)$$

where K is the perturbed Hamiltonian. Replacing K in Eq. (8) by its expression in $(\tilde{J}, \tilde{\psi})$ variables, and as this equation has now a stationary solution ($\partial F / \partial t = 0$), then the problem is reduced to

$$\begin{aligned} & \frac{\partial F}{\partial \tilde{\psi}} \left((\omega_s - \omega_m/3) - \frac{\omega_s \tilde{J}}{8} - \frac{\omega_s A_m \cos 3\tilde{\psi}}{16} (2\tilde{J})^{1/2} \right) \\ &= 2\kappa \tilde{J} \frac{\partial^2 F}{\partial \tilde{J}^2} + \frac{\partial F}{\partial \tilde{J}} \left(\frac{\omega_s A_m (2\tilde{J})^{3/2}}{16} \sin 3\tilde{\psi} + 2\gamma_d \tilde{J} + 2\kappa \right) \\ &+ 2\gamma_d F. \end{aligned} \quad (9)$$

We are interested in the part that contains the $\partial / \partial \tilde{J}$ derivatives. The separation needs to fix the variable $\tilde{\psi} = \tilde{\psi}_1$ in the rotating frame, and using factorization [$F(\tilde{J}, \tilde{\psi}) = g(\tilde{\psi}) \times h(\tilde{J})$], the equation can be written as

$$a(\tilde{J}) \frac{\partial^2 h}{\partial \tilde{J}^2} + b(\tilde{J}) \frac{\partial h}{\partial \tilde{J}} + c(\tilde{J}) h = 0, \quad (10)$$

where

$$\begin{aligned} a(\tilde{J}) &= 2\kappa \tilde{J}, \\ b(\tilde{J}) &= 2 \left[\frac{\omega_s A_m (2\tilde{J})^{3/2}}{32} \sin 3\tilde{\psi}_1 + \gamma_d \tilde{J} + \kappa \right], \\ c(\tilde{J}) &= 2\gamma_d. \end{aligned}$$

If the amplitude of the third-integer modulation is equal to zero, we find the well-known Haissinski steady state solution, where h describes a Gaussian bunch:

$$h(\tilde{J}) = \frac{\gamma_d}{\kappa} e^{-(\gamma_d/\kappa)\tilde{J}} \quad \text{or} \quad h(\phi, \delta) = \frac{\gamma_d}{\kappa} e^{-(\gamma_d/\kappa)[(\phi^2 + \delta^2)/2]}.$$

Finally, the bunch shape, given by the distribution $h(\tilde{J})$, will get the form: $A(\tilde{J})e^{-b(\tilde{J})/a(\tilde{J})}$ [where $A(\tilde{J})$ is an amplitude term coming from the solution of Eq. (10)].

The relevant term $b(\tilde{J})$, which contains the third-integer resonance perturbation with the synchrotron radiation effect, will determine the bunch Gaussian shape or the shape modulated by island formation. Thus the rf phase modulation is still efficient if the magnitude of the first coefficient is larger than the two last coefficients.

B. Island formation criterion

The three coefficients of the bracketed term of $b(\tilde{J})$ are

$$C_1 = \frac{\omega_s A_m (2\tilde{J})^{3/2}}{32} \sin 3\tilde{\psi}_1, \quad C_2 = \gamma_d \tilde{J}, \quad C_3 = \kappa.$$

The C_3 term, generally much smaller than C_1 and C_2 , can be neglected for phase space only.

When the modulation parameters are optimized to catch the particles located in the bunch core (1σ), it is particularly interesting to estimate if the particles are attracted into the islands or if they remain near the origin. With physical phase space variables (ϕ, δ) , and the assumption that 1σ particles are treated, then the coefficients can be written as

$$C_1 = \frac{\omega_s A_m}{16} \left(\frac{\alpha h \sigma_\epsilon}{Q_s} \right)^3, \quad C_2 = \frac{1}{T_{rad}} \left(\frac{\alpha h \sigma_\epsilon}{Q_s} \right)^2.$$

Expressing the perturbation amplitude A_m in σ units of the bunch, i.e., $A_m = a_m \sigma_\phi$, where a_m is an integer, we find a limit value of the radiation damping time for the formation of islands:

$$T_{rad} > \frac{16Q_s}{\omega_{RF} \alpha^2 h a_m \sigma_\epsilon^2}. \quad (11)$$

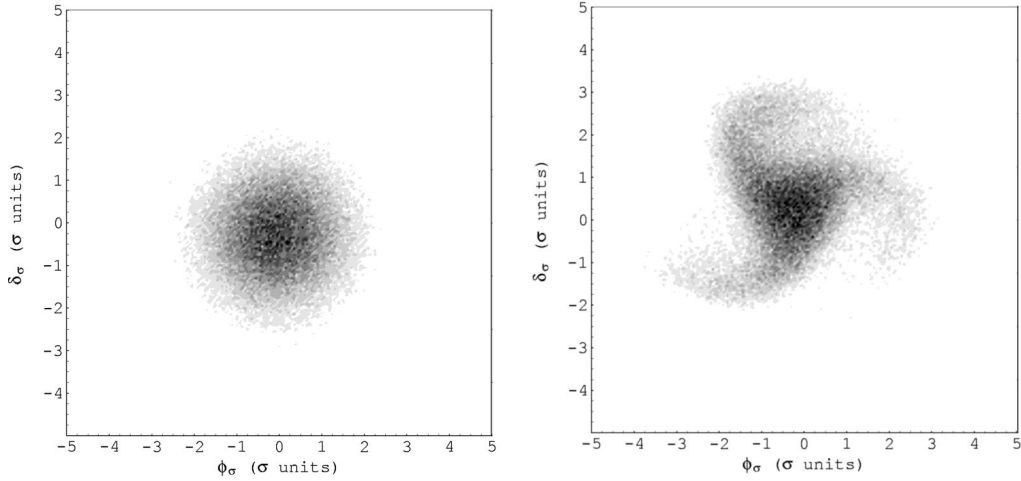


FIG. 7. Snapshots (10^5 particles) in normalized phase space $(\phi_\sigma, \delta_\sigma)$ with island destruction (left) and island formation (right) for SOLEIL. (a) SOLEIL: natural value of $\sigma_\epsilon = 9.24 \times 10^{-4}$. (b) SOLEIL: $\sigma_\epsilon = 15.0 \times 10^{-3}$ modified for island formation in agreement with the criterion limit.

Whenever the radiation damping time is larger, third-integer resonance dominates and islands will be formed.

C. Simulations of formation or destruction of islands

The validity of the island survival criterion has been checked for various parameters of the three specified previously machines with the help of a multiparticle tracking code, which simulates the motion of particles with rf phase modulation, synchrotron radiation, and quantum excitation. The simulation is based on the following recursive equations:

$$\phi_{n+1} = \phi_n + 2\pi Q_s \delta_n,$$

$$\delta_{n+1} = \left(1 - \frac{2}{T_{rad} F_0}\right) \delta_n + \frac{2}{\sqrt{T_{rad} F_0}} \sigma_\epsilon R_I - \frac{2\pi Q_s}{\cos \bar{\phi}_s} [\sin(\bar{\phi}_s + \phi_{n+1} + A_m \sin \omega_m t) - \sin \bar{\phi}_s], \quad (12)$$

where R_I is a random number of normal distribution and F_0 the revolution frequency.

For each calculation, the rf phase modulation parameters (ω_m, a_m) have first been optimized to get well-shaped islands. Furthermore, in order to shorten the simulation time for the criterion checking, it is preferable to use the energy spread parameter σ_ϵ instead of T_{rad} . Thus the criterion is now written as $\sigma_\epsilon > \sqrt{(1/T_{rad})(16Q_s/\omega_{RF}\alpha^2 h a_m)}$.

For each machine, island formation and destruction were looked for by using two values of energy spread: the natural

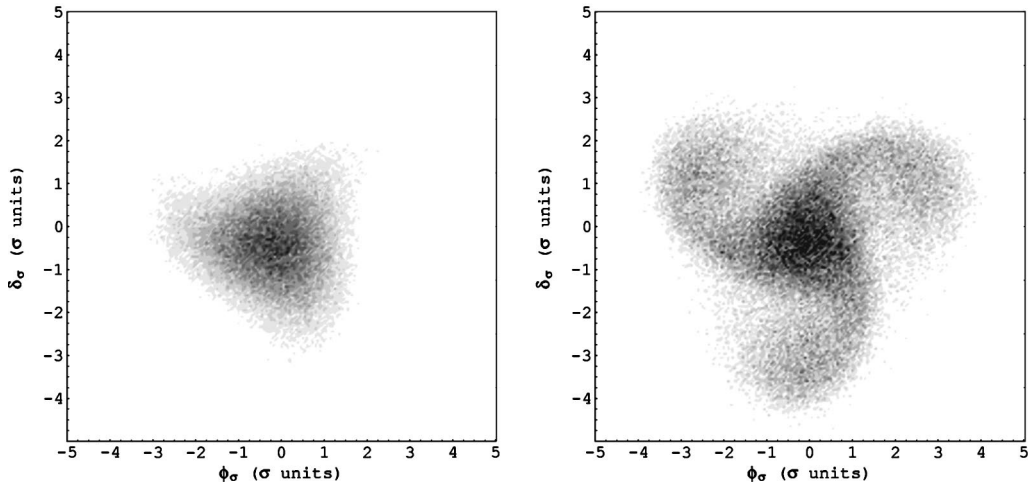


FIG. 8. Snapshots (10^5 particles) in normalized phase space $(\phi_\sigma, \delta_\sigma)$ with island destruction (left) and island formation (right) for BESSY I. (a) BESSY I: $\sigma_\epsilon = 2.3 \times 10^{-4}$ modified for island destruction in agreement with the criterion limit. (b) BESSY I: natural value of $\sigma_\epsilon = 5.0 \times 10^{-4}$.

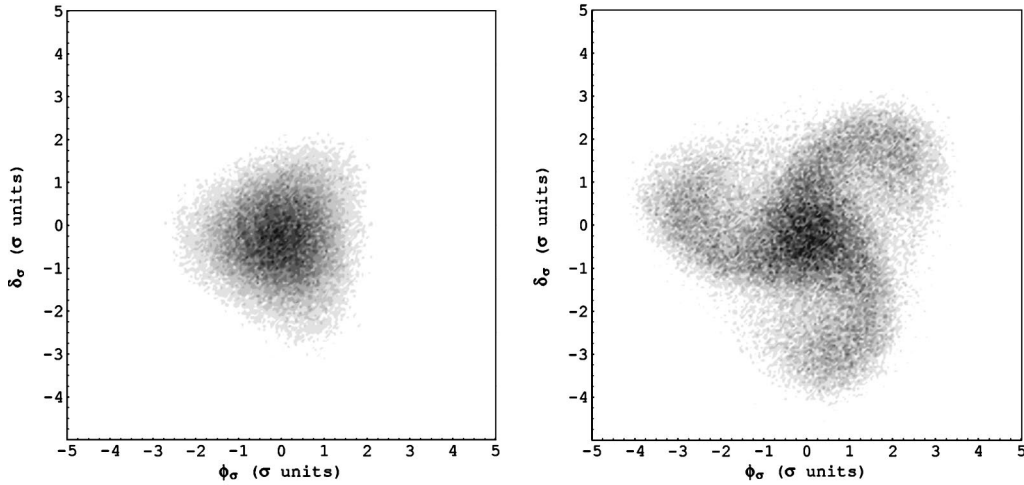


FIG. 9. Snapshots (10^5 particles) in normalized phase space $(\phi_\sigma, \delta_\sigma)$ with island destruction (left) and island formation (right) for SuperACO. SuperACO: natural value of $\sigma_\epsilon = 5.5 \times 10^{-4}$ for a bunch current equal to zero; there is island destruction in agreement with the criterion limit. (b) SuperACO: natural value of $\sigma_\epsilon = 18.33 \times 10^{-4}$ for a bunch current equal to 60 mA; there is island formation in agreement with the criterion limit.

one and a fictive one, giving the reverse situation. Figures 7, 8, and 9 give the particle distribution in phase space, showing the island destruction for SOLEIL [Fig. 7(a)] and SuperACO [Fig. 9(a)], and the island formation for BESSY I [Fig. 8(b)] with their natural energy spread. Table III summarizes the energy spread values, which were tested, as well as the limit value (natural energy spreads are in bold characters). The energy spread of SuperACO, that was chosen for island creation, is larger than the natural one, but corresponds nevertheless to a real situation, when the beam current is well above the turbulent regime.

It is worth noting that the required energy spread for island formation is much higher for the SOLEIL ring than for the other ones, due mainly to the low value of the momentum compaction. In addition, by assuming an energy spread larger than the limit value, chaotic motion and particle loss can be observed in Fig. 7, as predicted by the Chirikov criterion (cf. Table III).

Finally, Fig. 10 shows the enlarged charge distributions at different times, as well as the initial Gaussian distribution for comparison. Except for SOLEIL, the net bunch length has been increased by a factor between 2 and 3, but at the expense of a similar widening in energy spread, since islands are rotating in phase space at the modulation frequency ω_m .

V. CONCLUSION

With properly chosen parameters, the rf phase modulation method allows enlargement of the phase space occupied by

the beam. However, the energy spread is also increased, by the same bunch lengthening factor. The Touschek lifetime can then be increased by a factor of 2, as has been observed in BESSY I and ASTRID [6], but at the expense of beam quality, affecting in particular the brilliance in synchrotron light sources. In addition, the synchrotron radiation effect can prevent island formation in some cases, which can be predicted by a criterion on the minimum required energy spread.

APPENDIX

The properties of the Hamiltonian for synchrotron motion with rf phase modulation are discussed. The longitudinal phase space will be transformed to action-angle coordinates, where the Hamiltonian in the rotating frame will be derived. We explain why odd resonances only are considered and the complete perturbed Hamiltonian is calculated. Fixed point coordinates and island widths are derived in both frames (ϕ, δ) and $(\tilde{J}, \tilde{\psi})$.

1. The action-angle variables of the perturbed Hamiltonian (rf phase modulation with amplitude A_m and frequency ω_m)

$$\frac{d\phi}{dt} = \omega_s \times \delta,$$

$$\frac{d\delta}{dt} = -\frac{\omega_s}{\cos \phi_s} [\sin(\overline{\phi_s} + \phi + A_m \sin \omega_m t) - \sin \overline{\phi_s}].$$

TABLE III. σ_ϵ parameter of island formation or island absence due to the strong damping force.

	SOLEIL	BESSY I	SuperACO
$\sigma_\epsilon \text{ lim}$	11.13×10^{-3}	4.14×10^{-4}	14.02×10^{-4}
Island formation	$\sigma_\epsilon = 15.0 \times 10^{-3}$	$\sigma_\epsilon = 5.0 \times 10^{-4}$	$\sigma_\epsilon = 18.33 \times 10^{-4}$
$\omega_m \text{ chaos} / \omega_m \text{ modul}$	1.05	0.93	0.96
No island	$\sigma_\epsilon = 9.24 \times 10^{-4}$	$\sigma_\epsilon = 2.3 \times 10^{-4}$	$\sigma_\epsilon = 5.5 \times 10^{-4}$
$\omega_m \text{ chaos} / \omega_m \text{ modul}$	0.81	0.89	0.89

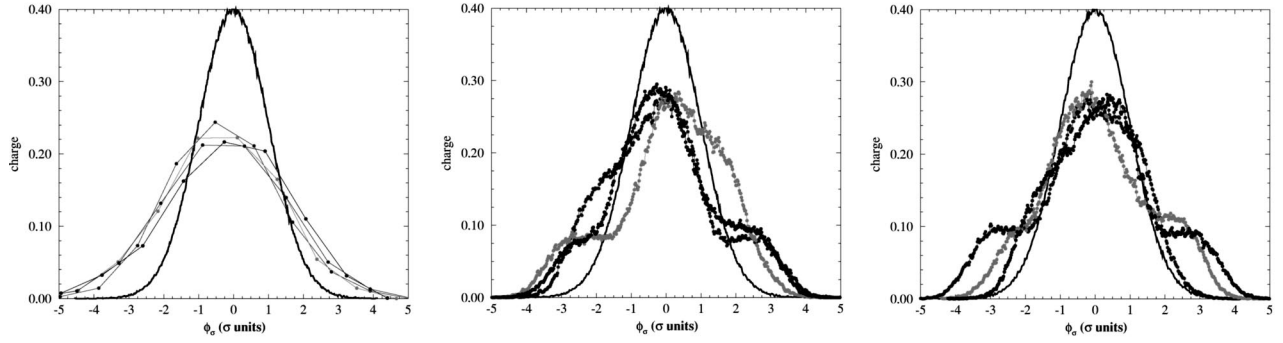


FIG. 10. Distribution in charge versus the normalized angle ϕ_σ of a bunch of 100 000 particles in situations where islands are formed. (a) SOLEIL: σ_ϵ modified. (b) Bessy I. (c) SuperACO.

The complete perturbed Hamiltonian in (ϕ, δ) variables is given by

$$\begin{aligned}
 H_1(\phi, \delta) = & \frac{\omega_s}{2} \delta^2 + \omega_s \tan \overline{\phi_s} [\sin \phi \cos(A_m \sin \omega_m t) \\
 & + \cos \phi \sin(A_m \sin \omega_m t)] \\
 & - \omega_s \cos \phi \cos(A_m \sin \omega_m t) \\
 & + \omega_s \sin \phi \sin(A_m \sin \omega_m t) - \omega_s \phi \tan \overline{\phi_s}.
 \end{aligned} \tag{A1}$$

The first canonical transformation in action-angle coordinates (J, ψ) gives the new Hamiltonian

$$\begin{aligned}
 H_1(J, \psi) = & \omega_s J \sin \psi^2 + \omega_s \tan \overline{\phi_s} \{ \sin[\sqrt{2J} \cos \psi \\
 & + A_m \sin(\omega_m t)] \} - \omega_s [\cos(\sqrt{2J} \cos \psi \\
 & + A_m \sin \omega_m t)] - \omega_s \tan \overline{\phi_s} (\sqrt{2J} \cos \psi).
 \end{aligned} \tag{A2}$$

The perturbed Hamiltonian is much more complicated and the perturbed part is not clearly defined. The Hamiltonian expanded into Bessel functions is written as

$$\begin{aligned}
 H_1(J, \psi) = & \omega_s J \sin \psi^2 - \omega_s J_o(\sqrt{2J}) - 2\omega_s \sum_{k=1}^{\infty} (-1)^k J_{2k}(\sqrt{2J}) \cos(2k\psi) - \omega_s \tan \overline{\phi_s} \sqrt{2J} \cos \psi \\
 & + \omega_s \tan \overline{\phi_s} A_m \sin(\omega_m t) J_o(\sqrt{2J}) + 2\omega_s \tan \overline{\phi_s} \sum_{k=0}^{\infty} (-1)^k J_{2k+1}(\sqrt{2J}) \cos[(2k+1)\psi] \\
 & + \omega_s A_m \sum_{k=0}^{\infty} (-1)^k J_{2k+1}(\sqrt{2J}) \{ \sin[\omega_m t \pm (2k+1)\psi]_{\text{odd resonances}} \} + \omega_s \tan \overline{\phi_s} A_m \\
 & \times \sum_{k=1}^{\infty} (-1)^k J_{2k}(\sqrt{2J}) [\sin(\omega_m t \pm 2k\psi)_{\text{even resonances}}].
 \end{aligned}$$

All resonances appear: the odd resonances $\sin[\omega_m t - (2k+1)\psi]$ and the even resonances $\sin(\omega_m t - 2k\psi)$ (terms with plus signs are nonresonant terms). All the terms containing $\tan \overline{\phi_s}$ are neglected in the following, because generally in storage rings bunches are placed for the maximum rf acceptance, so the synchronous phase $\overline{\phi_s} \rightarrow 0$. For this reason even resonances can be neglected compared to the odd ones.

2. Study of the third-integer resonance: $\omega_m \approx 3\omega_s$

Assuming that we are close to the third-integer resonance ($k=1$) and that all nonresonant terms in the Hamiltonian can be neglected, then the Hamiltonian becomes

$$\begin{aligned}
 H_1(J, \psi) = & \omega_s J - \frac{\omega_s J^2}{16} - \omega_s - \frac{\omega_s J}{2} \cos 2\psi - 2\omega_s \\
 & \times \sum_{k=1}^{\infty} (-1)^k J_{2k}(\sqrt{2J}) \cos(2k\psi) \\
 & - \omega_s A_m J_3(\sqrt{2J}) \sin(\omega_m t - 3\psi).
 \end{aligned}$$

H_1 is time dependent again. A new canonical transformation to a rotating system in phase space eliminates this dependence. A generating function of the second type is used for the new transformation:

$$F_2(\tilde{J}, \tilde{\psi}) = \left(\psi - \frac{\omega_m t}{3} - \frac{\pi}{2} \right) \tilde{J}$$

with $\tilde{J} = J$ and $\tilde{\psi} = \psi - \omega_m t/3 - \pi/2$.

The new Hamiltonian K is independent of time; thus it is a constant of motion:

$$K = H_1 + \frac{\partial F_2}{\partial t} = H_1 + \left(-\frac{\omega_m}{3} \right) \tilde{J}.$$

In the rotating frame, the particle trajectories are described by the total time-averaged Hamiltonian K :

$$\langle K \rangle_t = \left(\omega_s - \frac{\omega_m}{3} \right) \tilde{J} - \frac{\omega_s \tilde{J}^2}{16} - \frac{\omega_s A_m (2\tilde{J})^{3/2}}{48} \cos 3\tilde{\psi} - \omega_s. \quad (\text{A3})$$

Terms in the Hamiltonian that are not functions of \tilde{J} and $\tilde{\psi}$ do not affect the differential equations for \tilde{J} and $\tilde{\psi}$ and thus can be ignored in the following (ω_s is also neglected).

3. Fixed point calculation

These fixed points are obtained by the following conditions:

$$\begin{aligned} \frac{d\tilde{J}}{dt} = -\frac{\partial K}{\partial \tilde{\psi}} &= 0, \\ \frac{d\tilde{\psi}}{dt} = \frac{\partial K}{\partial \tilde{J}} &= 0. \end{aligned} \quad (\text{A4})$$

With both equations, six fixed points are found for which the sign of $\cos 3\tilde{\psi}$ determines their stability or the instability: (1) Three stable fixed points (SFPs) for $\tilde{\psi} = 0, 2\pi/3, 4\pi/3$. They are stable because the term $\cos 3\tilde{\psi}$ is positive and the potential has a minimum. (2) Three unstable fixed points (UFPs) for $\tilde{\psi} = \pi/3, \pi, 5\pi/3$. They are unstable because the term $\cos 3\tilde{\psi}$ is negative and the potential has a maximum.

The trajectories surrounding the stable fixed points are closed and form islands of stability for particles, whereas the trajectories surrounding the UFPs are hyperbolic and these curves are separatrices, which are the boundaries of the stable islands. In the new phase space $(\tilde{J}, \tilde{\psi})$, the stationary trajectories correspond to the K -constant contours.

The coordinates $(\phi_\sigma, \delta_\sigma)$ of the three stable fixed points are (for $\tilde{\psi} = 0, 2\pi/3, 4\pi/3$)

$$\delta_\sigma = \frac{a_m}{2}(1 + R_{FP}), \quad -\frac{a_m}{4}(1 + R_{FP}), \quad -\frac{a_m}{4}(1 + R_{FP}),$$

$$\phi_\sigma = 0, \quad \sqrt{3} \frac{a_m}{4}(1 + R_{FP}), \quad -\sqrt{3} \frac{a_m}{4}(1 + R_{FP}). \quad (\text{A5})$$

The coordinates $(\phi_\sigma, \delta_\sigma)$ of the three unstable fixed points are

$$\delta_\sigma = -\frac{a_m}{2}(1 - R_{FP}), \quad -\frac{a_m}{4}(1 - R_{FP}), \quad -\frac{a_m}{4}(1 - R_{FP}),$$

$$\phi_\sigma = 0, \quad \sqrt{3} \frac{a_m}{4}(1 - R_{FP}), \quad -\sqrt{3} \frac{a_m}{4}(1 - R_{FP}), \quad (\text{A6})$$

with the the factor $R_{FP} = \sqrt{1 + (64Q_s^2/a_m^2)(\sigma_\epsilon h \alpha)^2}(1 - \omega_m/3\omega_s)$, where a_m is the normalized modulation amplitude (A_m is in units of rms bunch length), Q_s is the synchrotron tune, σ_ϵ is the natural energy spread, α is the momentum compaction, and h is the harmonic number. When ω_m tends to $3\omega_s$, the UFP coordinates are canceled.

4. Island width calculation

The boundaries of the stable islands are formed by curves joining the unstable fixed points. As K is a constant of the curve, we can write $K(\tilde{J}, \tilde{\psi}) = K(\tilde{J}_{UFP}, \tilde{\psi}_{UFP})$ where \tilde{J}_{UFP} is the action at the unstable fixed points; also on the separatrix we find

$$(\tilde{J} - \tilde{J}_{UFP})^2 \simeq \frac{A_m [16(1 - \omega_m/3\omega_s)]^{3/2} (1 + \cos 3\tilde{\psi})}{3}. \quad (\text{A7})$$

The island width $\Delta\tilde{J}$ is given by the distance between the separatrix and the stable fixed points, where the Hamiltonian is maximum [3]:

$$\Delta\tilde{J} = \pm 8 \sqrt{\frac{A_m 2(1 - \omega_m/3\omega_s)^{3/2}}{3}}.$$

For the easiest stable fixed point, where $\tilde{\psi} = 0$, and with a change in variable, $\Delta\tilde{J} = (\tilde{J}_{SFP} - \tilde{J}_{UFP}) = (\delta_{SFP}^2 - \delta_{UFP}^2)/2$ and $\delta_{SFP}^2 - \delta_{UFP}^2 = (\delta_{SFP} - \delta_{UFP})(\delta_{SFP} + \delta_{UFP}) = \Delta\delta(\delta_{SFP} + \delta_{UFP})$, then the island width in phase space coordinates is

$$\Delta\delta = \pm 16 \sqrt{\frac{A_m 2(1 - \omega_m/3\omega_s)^{3/2}}{3}} \frac{1}{\delta_{SFP} + \delta_{UFP}}.$$

The island width, normalized in σ units and expressed with storage ring parameters, is

$$\Delta\delta_\sigma = \pm 16 \sqrt{\frac{2}{3}} \left(\frac{Q_s}{\alpha \sigma_\epsilon h} \right)^{3/2} (1 - \omega_m/3\omega_s)^{3/4} \frac{1}{\sqrt{a_m} R_{FP}}. \quad (\text{A8})$$

Generally, $(64Q_s^2/a_m^2)(\sigma_\epsilon h \alpha)^2(1 - \omega_m/3\omega_s) \gg 1$, thus we can approximate Eq. (A8), so we obtain

$$\Delta\delta_\sigma \simeq \pm 2 \sqrt{\frac{2}{3}} \left(\frac{Q_s}{\alpha \sigma_\epsilon h} \right)^{1/2} (1 - \omega_m/3\omega_s)^{1/4} \sqrt{a_m}. \quad (\text{A9})$$

The island width grows with a_m , but it is reduced when ω_m tends to $3\omega_s$ [$\Delta\delta_\sigma \propto (1 - \omega_m/3\omega_s)^{1/4}$].

- [1] V.V. Balandin, M.B. Dyachkov, and E.N. Shaposhnikova, *Part. Accel.* **35**, 1 (1991).
- [2] H. Huang *et al.*, *Phys. Rev. E* **48**, 4678 (1993).
- [3] R.D. Ruth, in *Lecture Notes in Physics Vol. 247* (Springer-Verlag, Berlin, 1985).
- [4] B.V. Chirikov, *Phys. Rep.* **52**, 1 (1979).
- [5] P. Kuske, Yu. Senichev, and M.P. Level (private communication).
- [6] Yu. Senichev, N. Hertel, S. Lunt, S.P. Moeller, and J.S. Nielsen, in *Proceedings of the European Particle Accelerator Conference, Stockholm, 1998*, edited by S. Meyers (Institute of Physics, Bristol, 1998), p. 1339.